Title
ENERGY LEVELS OF Bi210 AND Po210 AND THE SHELL-MODEL RESIDUAL FORCE

Authors
Kim, Yeong E.
Rasmussen, John O.

Publication Date
1963-03-11

UCRL-10707

University of California

Ernest O. Lawrence Radiation Laboratory

ENERGY LEVELS OF Bi^{210} AND Po^{210} AND THE SHELL-MODEL RESIDUAL FORCE

Berkeley, California

DISCLAIMER

Submitted to Nuclear Physics

UCRL-10707 errata

UNIVERSITY OF CALIFORNIA
Lawrence Radiation Laboratory
Berkeley, California

Contract No. W-7405-eng-48

ENERGY LEVELS OF Bi^{210} AND Po^{210} AND THE SHELL-MODEL RESIDUAL FORCE

Yeong E. Kim and John O. Rasmussen

March 11, 1963

UNIVERSITY OF CALIFORNIA

Lawrence Radiation Laboratory
Berkeley, California

Contract No. W-7405-eng-48

April 17, 1963

ERRATA

TO: All recipients of UCRL-10707

FROM: Technical Information Division

Subject: UCRL-10707, "Energy Levels of Bi^{210} and Po^{210} and the Shell-Model Residual Force," Yeong E. Kim and John O. Rasmussen,

Page	Line	As it is	Should read
4	15	-	+
6	3	$[- 1 - (-1) \cdots$	$- [1 - (-1) \cdots$
8	6	$(\underset{\sim}{r}^{12})S_{12}\|\alpha' J_1' M'\rangle$	$(\underline{r}_{12})S_{12}\|\alpha' j_1' j_2' J' M'\rangle$
8	11	j'M'	J'M'

All $\underset{\sim}{r}_{12}$ appearing in $V(\underset{\sim}{r}_{12})$ and $U(\underset{\sim}{r}_{12})$ should be replaced by $\underline{r}_{12}$.

ENERGY LEVELS OF Bi^{210} AND Po^{210} AND THE SHELL-MODEL RESIDUAL FORCE

Yeong E. Kim and John O. Rasmussen

Lawrence Radiation Laboratory
University of California
Berkeley, California

March 11, 1963

ABSTRACT

The low-lying energy-level spectra of Bi^{210} and Po^{210} are calculated by using the j-j coupling shell-model and a residual nucleon-nucleon Gaussian potential without a hard core deduced from the free two-nucleon potentials of Blatt-Jackson and Brueckner-Gammel-Thaler. The spin-orbit force is neglected, but all direct and exchange components of the central and tensor forces are considered. Tensor-force effects are examined as a function of the range. A tensor force with reasonable range and strength accounts for the 1- state of the $h_{9/2}\, g_{9/2}$ multiplet being the ground state of Bi^{210}, instead of the 0- predicted by central forces. Eigenvalues and eigenfunctions are presented and compared with the experimental spectra. Finally it is shown that the ground-state wave functions for Bi^{210} and Po^{210} are consistent with the RaE β-decay parameter $i\langle \underset{\sim}{r} \rangle / \langle \underset{\sim}{\sigma} \times \underset{\sim}{r} \rangle$ and the measured magnetic dipole moment of Bi^{210}.

ENERGY LEVELS OF Bi^{210} AND Po^{210} AND THE SHELL-MODEL RESIDUAL FORCE†

Yeong E. Kim and John O. Rasmussen

Lawrence Radiation Laboratory
University of California
Berkeley, California

March 11, 1963

1. Introduction

The low-lying energy-level spectrum of Bi^{210} has been the object of several shell-model theoretical studies[1]. The nucleus has one proton and one neutron beyond the doubly closed-shell nucleus Pb^{208}, and the lowest proton orbital is $h_{9/2}$ and the lowest neutron orbital $g_{9/2}$. One thus expects a low-lying multiplet of ten levels with spins from zero to nine for Bi^{210}. With the experimental determination eight years ago of a ground-state spin of one, a difficult problem was posed for shell-model theory, for almost any reasonable attractive central-force mixture acting between the neutron and proton bring spin 0 lower than spin 1, whereas experimentally spin 0 lies 47 keV higher.

The inversion of 0- and 1- states of the $h_{9/2}\, g_{9/2}$ configuration in Bi^{210} is a striking exception to Nordheim's "strong"-coupling rule for odd-odd nuclei. To explain this inversion, Newby and Konopinski[1] and Kharitonov, Sliv, and Sogomonova[2] attribute the 1- state to the configuration $h_{9/2}\, i_{11/2}$. More recently the study by de-Shalit and Walecka of the angular ordering function suggested that the inversion of 0- and 1- states of $h_{9/2}\, g_{9/2}$ may be explained with a proper choice of the central-force range[3]. Newby and Konopinski gave qualitative arguments that an attractive tensor force would be repulsive for the 0- state and help force it up.

Now the low-energy, high-resolution (d,p) reaction studies of Erskine et al. on Bi^{209} present a wealth of new information on the $h_{9/2}\ g_{9/2}$ multiplet[4] and necessitate a thorough reexamination of the shell-model theory. They resolve nine of the expected ten levels of the $h_{9/2}\ g_{9/2}$ multiplet and make tentative spin assignments on the basis that the reaction cross sections are proportional to 2I+1. Furthermore, they see higher multiplets attributable to capture of the neutrons into $d_{5/2}$ and $s_{1/2}$ excited orbitals. The multiplets arising from capture into $i_{11/2}$ or $j_{15/2}$ orbitals are weak and not resolved completely, presumably because the high orbital-angular-momentum transfers are strongly discriminated against in the (d,p) reaction.

Figure 1 shows Erskine's spectrum with indicated level numbers. The spins are assigned in sequence of J = 1, 0, 9, 2, 3, 5 and 8 (or 5 and 7), 4, 6, and 7 (or 8) with corresponding level numbers 0, 1, 2, 3, 5, 6, 7, and 8. These results strongly indicate that the ground state involves mainly the $g_{9/2}$ neutron orbital and not the $i_{11/2}$. Erskine made shell-model calculations with a finite Gaussian Serber force (central-even components only) as a function of range[5]. He took a ratio of 0.66 for singlet-to-triplet strength, which free-space two-body scattering and other shell-model work indicate is reasonable. At a force range of 2.7 fm he finds a fairly good fit for all except the spin-0 and -1 levels, which are inverted from their experimental order.

The spectrum of Po^{210} was theoretically calculated by Hoff and Hollander[6] with a delta-function force, and by Newby and Konopinski with a central singlet-even force, which is reasonable from the free two-nucleon potential. We also shall treat the Po^{210} spectrum to see the effects of a tensor force and to determine if one can explain the spectra of both Bi^{210}

and Po^{210} with the same residual force. The experimentally observed low-lying energy levels in Bi^{210} and Po^{210} are presented in fig. 2.

2. The Shell-Model Calculation and Central-Force Effects

Before discussing the tensor-force effects in detail, we describe the basic assumptions that enter into our calculation. We assume that Pb^{208} can be treated as an inert core providing a harmonic-oscillator potential well for the extra nucleons. There are two nucleons outside this doubly closed shell in Bi^{210} and Po^{210}. Sliv et al. have included the effects of Pb^{208} core excitation of a quadrupole surface-oscillation type. It generally appears from their work that such a refinement brings an important enhancement of E2 transition probabilities, but that the relative level spacings for low-lying levels are not greatly altered.

Basis vectors are products of our harmonic-oscillator function for particles 1 and 2, coupled to a total angular momentum J:

$$|a\rangle = R_1(r_1)R_2(r_2)|j_1 j_2 JM\rangle .$$

It is understood that these vectors must be antisymmetrized for Po^{210}, since Po^{210} involves two identical particles (protons). In our j-j-coupled odd-group model, the Hamiltonian describing these nuclei at low energy is assumed to be written as

$$H = H_1 + H_2 + V_{12} ,$$

where H_1 and H_2 are the single-particle Hamiltonians and V_{12} is the residual interaction between particles 1 and 2. We assume that H_i acting on our wave function yields

$$H_i |a\rangle = \epsilon_0^i |a\rangle ,$$

for $i = 1, 2$, where ϵ_0^i are the single-particle energies for the particle i. The sum of the single-particle energies ϵ_0^1 and ϵ_0^2 will be the zero-order energy. The independent-particle energies are taken from the neighboring nuclei Pb^{209} and Bi^{209}, and the resulting zero-order energies are listed in table 1. Recently seven single-particle levels for the neutron in Pb^{209} have been reported by Cohen et al.[7].

The residual force V_{12} splits the degeneracy of the independent-particle states and also brings in configuration mixing. In the usual fashion we obtain the state energies W from the solutions of the set of eigenvalue equations for each I value:

$$\sum_{a'} \left[\langle a | V_{12} | a' \rangle - (W - \epsilon_{0a'}) \delta_{aa'} \right] \langle a' | aJM \rangle = 0$$

The summation is restricted to the configuration listed in table 1.

The residual two-body interaction V_{12} is expressed generally as

$$V_{12} = V^C(r_{12}) - V^T(r_{12}) S_{12} ,$$

where the first term is the central force, and the second term is the tensor force. Considering space and spin exchange we have four components of the central force,

$$V^C(r_{12}) = \left[V_{TE}^{\ C} P_{TE} \exp (-\beta_{TE}^{\ C} r_{12}^2) \right.$$

$$+ V_{SE}^{\ C} P_{SE} \exp (-\beta_{SE}^{\ C} r_{12}^2)$$

$$\left. + V_{TO}^{\ C} P_{TO} \exp (-\beta_{TO}^{\ C} r_{12}^2) \right.$$

$$+ V_{SO}{}^{C} P_{SO} \exp\left(-\beta_{SO}{}^{C} r_{12}{}^{2}\right) \Big] ,$$

and two components (triplet spin states only) of the tensor force,

$$V^{T}(r_{12}) = \Big[V_{TE}{}^{T} P_{TE} \exp\left(-\beta_{TE}{}^{T} r_{12}{}^{2}\right)$$

$$+ V_{TO}{}^{T} P_{TO} \exp\left(-\beta_{TO}{}^{T} r_{12}{}^{2}\right) \Big] .$$

where P_{TE}, P_{SE}, P_{TO}, and P_{SO} are the projection operators for the triplet-even, singlet-even, triplet-odd, and singlet-odd states, respectively, and V's are the corresponding strength parameters. The operator S_{12} is the tensor-force operator defined as

$$S_{12} = \frac{3(\sigma_1 \cdot r_{12})(\sigma_2 \cdot r_{12})}{r_{12}^{2}} - \sigma_1 \cdot \sigma_2 .$$

The harmonic-oscillator radial function will be used throughout the numerical calculations for the radial integrals. The size parameter $(\nu)^{-1/2}$ appearing in the wave function as $\psi \sim e^{-\nu r^{2}/2}$ is determined from the harmonic-oscillator spacing, which is roughly given by

$$\hbar\omega = \frac{\hbar^{2}\nu}{m} = 41\, A^{-1/3} \text{ MeV}.$$

The central-force matrix elements can be expressed as

$$\langle a|V^{C}(r_{12})|a'\rangle = \frac{1}{2} V_{TE}{}^{C} \Big\{ \Big[1 + (-1)^{j_1'+j_2'+J} P'_{12} \Big] \langle a|U_{TE}{}^{C}(r_{12})|a'\rangle$$

$$- \Big[1 + (-1)^{j_1'+j_2'+J} P'_{12} \Big] \langle a|U_{TE}{}^{C}(r_{12})|a'\rangle \Big\}$$

$$+ \frac{1}{2} V_{SE}{}^{C} \left\{ \left[1 - (-1)^{j_1'+j_2'+J} P'_{12} \right] \langle a | U_{SE}{}^{C}(r_{12}) P_S | a' \rangle \right\}$$

$$+ \frac{1}{2} V_{TO}{}^{C} \left\{ \left[1 - (-1)^{j_1'+j_2'+J} P'_{12} \right] \langle a | U_{TO}{}^{C}(r_{12}) | a' \rangle \right\}$$

$$\left[- 1 - (-1)^{j_1'+j_2'+J} P'_{12} \right] \langle a | U_{TO}{}^{C}(r_{12}) P_S | a' \rangle \Big\}$$

$$+ \frac{1}{2} V_{SO}{}^{C} \left\{ \left[1 + (-1)^{j_1'j_2'+J} P'_{12} \right] \langle a | U_{SO}{}^{C}(r_{12}) P_S | a' \rangle \right\} ,$$

where P_S is the singlet projection operator, and operator P'_{12} acts only on the initial states and is defined as $P'_{12} | j_1' j_2' \, JM \rangle = | j_2' j_1' \, JM \rangle$.

The matrix elements $\langle a | U^{C}(r_{12}) | a' \rangle$ and $\langle a | U^{C}(r_{12}) \, P_S | a' \rangle$ are given in the j-j representation as (see reference 9 for detail)

$$\langle a | U^{C}(r_{12}) | a' \rangle = (-1)^{j_a'+j_2+J} ([j_1][j_2][j_1'][j_2'])^{1/2}$$

$$\times \sum_k F_k(j_1' \; \tfrac{1}{2} \; j_1 - \tfrac{1}{2} | k0)(j_2' \; \tfrac{1}{2} \; j_2 - \tfrac{1}{2} | k0) W(j_1 j_1' j_2 j_2' ; kJ) ,$$

with the restriction that $k + \ell_1 + \ell_1'$ and $k + \ell_2 + \ell_2'$ are both even, and the symbol $[a]$ stands for $[2a + 1]$, and

$$\langle a | U^{C}(r_{12}) P_S | a' \rangle = (-1)^{j_2'+j_2+J-1} ([j_1][j_2][j_1'][j_2'])^{1/2} ([\ell_1][\ell_2][\ell_1'][\ell_2'])^{1/2}$$

$$\times W(\ell_1 j_1 \ell_2 j_2 ; \tfrac{1}{2} \, J) W(\ell_1' j_1' \ell_2' j_2' ; \tfrac{1}{2} \, J)$$

$$\times \sum_k F_k(\ell_1 0 \ell_1' 0 | k0)(\ell_2 \; 0 \; \ell'_2 \; 0 | k0) W(\ell_1 \ell_1' \ell_2 \ell_2' ; kJ).$$

The Slater integral F_k is defined

$$F_k = \int_0^\infty R_1(r_1)R_1'(r_1)r_1^2 dr_1 \int_0^\infty R_2(r_2)R_2'(r_2)r_2^2 dr_2$$

$$\times \int_{-1}^{1} d\left(\frac{\cos\omega_{12}}{2}\right) P_k(\cos\omega_{12}) U^C(r_{12}) ,$$

where $U^C(r_{12})$ takes the Gaussian form $\exp(-\beta r_{12}^2)$ with different values of β for the corresponding states.

If one investigates the effects of the four central-force components separately, one finds that a central-force mixture cannot explain the inversion without losing the agreement on positions of other levels. The triplet-even central force which should be attractive and strongest of the components always brings the 0- state below the 1- state in energy. Although the triplet-odd part yields significantly large matrix elements similar to those for the triplet-even, we expect the triplet-odd matrix elements to be very small compared to the triplet-even contribution since the triplet-odd strength is known to be very weak from the free-space two-nucleon potential. The above arguments are seen by examination of fig. 3, which is a plot of the magnitude of diagonal matrix elements for $h_{9/2}\, g_{9/2}$ multiplet states. From fig. 3, it is clear that a reasonable central force, predominantly attractive triplet even, can explain most of the levels of the $h_{9/2}\, g_{9/2}$ multiplet except the inversion of the 0- and 1- states and that it is very difficult to adjust the force parameters so as to invert the 0- and 1- states without disturbing the sequence of other spin states in the $h_{9/2}\, g_{9/2}$ configuration. At this point we feel it most important to quantitatively evaluate the tensor-force matrix elements with a realistic radial dependence.

3. Tensor-Force Effects

The tensor force has been evaluated in terms of spherical tensors by Talmi[8]. The tensor-force matrix element can be conveniently expressed in either the L-S representation[1] or the j-j representation[3,9]. In the j-j representation, the matrix element for the tensor force is

$$\langle \alpha j_1 j_2 JM | V^T(\underset{\sim}{r}^{12}) S_{12} | \alpha' J_1' M' \rangle = \tfrac{1}{2} V_{TE}{}^T \Big[\langle \alpha j_1 j_2 JM | U_{TE}{}^T(\underset{\sim}{r}_{12}) S_{12} | \alpha' j_1' j_2' J' M' \rangle$$

$$+ (-1)^{j_1'+j_2'+J} \langle \alpha j_1 j_2 JM | U_{TE}{}^T(\underset{\sim}{r}_{12}) S_{12} | \alpha' j_2' j_1' J' M' \rangle \Big]$$

$$+ \tfrac{1}{2} V_{TO}{}^T \Big[\langle \alpha j_1 j_2 JM | U_{TO}{}^T(\underset{\sim}{r}_{12}) S_{12} | \alpha' j_1' j_2' J' M' \rangle$$

$$+ (-1)^{j_1'+j_2'+J} \langle \alpha j_1 j_2 JM | U_{TO}{}^T(\underset{\sim}{r}_{12}) S_{12} | \alpha' j_2' j_1' J' M' \rangle \Big],$$

and

$$\langle \alpha j_1 j_2 JM | U^T(\underset{\sim}{r}_{12}) S_{12} | \alpha' j_1' j_2' j' M' \rangle = \sum_{K,x,y} \langle \alpha | F_{xy} | \alpha' \rangle W(1x\ 1y; K2)$$

$$\times \langle j_1 j_2 JM | \overline{T}_1(1x)K \cdot \overline{T}_2(1y)K | j_1' j_2' J' M' \rangle .$$

Here we define

$$\langle \alpha | F_{xy} | \alpha' \rangle = -5 \sum_{k,i,j} \langle \alpha | r_i r_j | \alpha' \rangle X_{ij} , \qquad \text{for } i, j = 1, 2$$

$$X_{11} = \left(\frac{2}{15} [x] \right)^{1/2} (20k0 | x0),$$

$$X_{22} = \left(\frac{2}{15}\,[y]\right)^{1/2}(20k0|yo)\ ,$$

$$X_{12} = ([x][y])^{1/2}\ (10k0|x0)(10k0|yo)W11xy;2k)\ ,$$

and

$$\langle \alpha|r_i r_j|\alpha'\rangle = (2k+1)\int_0^\infty dr_1 r_1{}^2 R_1 R_1{}' \int_0^\infty dr_2 r_2{}^2 R_2 R_2' r_i r_j$$

$$\times \int_{-1}^{1} d\left(\frac{\cos\omega_{12}}{2}\right)\ P_k(\cos\omega_{12})\ \frac{U^T(r_{12})}{r_{12}{}^2}\ ,$$

where $U^T(r_{12})$ takes the Gaussian form

$$U_{TE}{}^T(r_{12}) = \exp(-\beta_{TE}{}^C\ r_{12}{}^2)$$

for the triplet-even, and

$$U_{TO}{}^T\ (r_{12}) = \exp\ (-\beta_{TO}{}^C\ r_{12}{}^2)$$

for the triplet-odd. The angular part in terms of the 3-, 6-, and 9-j symbols is

$$\langle j_1 j_2 JM|\bar{T}_1{}^{(1x)K}\cdot\bar{T}_2{}^{(1y)K}|j_1' j_2' JM\rangle = (-1)^{j_1'+j_2+\ell_1+\ell_2+J}\,6\,\delta_{JJ'}\,\delta_{MM'}\begin{Bmatrix} J & j_2 & j_1 \\ k & j_1' & j'_2 \end{Bmatrix}$$

$$\times\ ([j_1][j_2][j_1'][j_2'])^{1/2}\ ([\ell_1][\ell_2][\ell_1'][\ell_2'])^{1/2}$$

$$\times \begin{pmatrix} \ell_1 & x & \ell_1' \\ 0 & 0 & 0 \end{pmatrix} \begin{pmatrix} \ell_2 & y & \ell_2' \\ 0 & 0 & 0 \end{pmatrix} \begin{Bmatrix} \frac{1}{2} & \frac{1}{2} & 1 \\ \ell_1' & \ell_1 & x \\ j_1' & j_1 & K \end{Bmatrix} \begin{Bmatrix} \frac{1}{2} & \frac{1}{2} & 1 \\ \ell_2' & \ell_2 & y \\ j_2' & j_2 & K \end{Bmatrix} .$$

The detail of the derivation of this expression and the method of evaluating the radial integral are presented elsewhere[9].

The above expression for the tensor-force matrix element is still sufficiently complicated so that it is very difficult to draw any conclusions before doing the numerical work. Figures 4, 5, 6, and 7 present the results for the diagonal contribution of the tensor-even and tensor-odd forces on the $h_{9/2}\ g_{9/2}$ multiplet as a function of the range parameter. These results confirm the qualitative predictions of Newby and Konopinski; for an attractive tensor force both even and odd components are quite repulsive for the spin-0 state. At the ranges comparable to the free-space ranges of Gammel-Thaler, the tensor force affects the spin-1 in an opposite sense to the spin-0 state, and it has only a rather small effect on the states of spin 2 or higher.

As shown in the figures, the tensor-force matrix elements are not always a monotonically increasing function of the range, and they may be either positive or negative in contrast to the central-force matrix elements. Thus the shorter-range tensor-force matrix elements are in quite different ratios to one another than in the infinite-range limit. This implies that the infinite-range approximation for the tensor force is not very realistic for shell-model calculations.

4. Numerical Calculations for Bi^{210} and Po^{210}

Because we set out to make a shell-model calculation with a residual force more general than usually used, we face the problem of essentially more parameters than data. With each of four central-force and two tensor-force components are two parameters, depth and range of the Gaussian function, or twelve parameters in all. For Po^{210}, half these components are not operative, because of the exclusion principle. However, the more extensive and critical data are the energies of the $(h_{9/2}\ g_{9/2})$ multiplet in Bi^{210}, and all six force components may be operative. Our earliest calculations concentrated on Bi^{210}, and we adopted the approach that we would begin calculations with residual forces close to those satisfying the free-space two-nucleon scattering data and deuteron properties. If necessary, we would then make a minimum of adjustments to the force to give a general fit to the experimental-level spectra.

It has often been pointed out that the free-space nucleon-nucleon force may be subject to modification for shell-model calculations, but as yet there seems to be no strong evidence that large modifications necessarily occur. In fact, there are successful shell-model calculations of Dawson, Talmi, and Walecka[10] on the O^{18} spectrum using the Brueckner-Gammel-Thaler (BGT) potentials[11] including the tensor force and hard cores. Their results lend encouragement to our approach.

Introduction of a hard core along with Yukawa raidal dependence would have made our computational work extremely complex. This is especially true for a heavy nucleus which involves higher angular momenta. For this reason we start with a phenomenological Gaussian potential without a hard core, deduced from the free two-nucleon potentials of

Brueckner, Gammel and Thaler and of Blatt and Jackson[12]. We use the well-depth parameter and intrinsic range defined by Blatt and Jackson in the shape-independent approximation of the effective-range theory to replace the Yukawa radial dependence with a hard core (the BGT potential) by a Gaussian form without a hard core. To reduce the number of adjustable parameters, we arbitrarily take the intrinsic ranges of our potential to be same as the BGT potential. From shape-independent, effective-range theory, the force range $\beta^{-1/2}$ of a Gaussian potential is larger by a factor of 1.477 than the force range of a Yukawa potential, such as the BGT potential. The well-depth parameters of our potential are expected to be smaller than those of the BGT potential since the introduction of a repulsive hard core always requires the attractive Yukawa potential to be deeper than for no core.

Note in table 2 that the first-approximation force for our calculations (Potential I) has Gaussian range parameters (1/e distance) just 1.477 times the 1/e distance for the BGT Yukawa potential. Somewhat arbitrarily we set the central-triplet-even strength at -223.02 MeV, which would by itself cause the deuteron to have zero binding energy. The factor 3.93 between the BGT strength parameter (-877.39 MeV) and our strength parameter was then applied to reduce all other components of the force. Kalos et al. have calculated deuteron properties and scattering properties with Gaussian forces and showed that several combinations of central and tensor strengths and ranges could fit the data[13]. The triplet components of our Potential I are fairly close to an interpolation of two of their satisfactory potentials, so we feel that our Potential I would be consistent with free-space properties of the n-p system.

The Po^{210} calculations gave somewhat too close spacing of the lowest 2+, 4+, 6+ level grouping. Their spacing seemed relatively insensitive to details of configuration mixing and to the tensor-force strength. Therefore, the central singlet-even force component seemed somewhat too weak and was strengthened by about 20% in the adjusted Potential II. It should be noted that the singlet-even part of the Potential I gives zero binding energy for a free-space, two-nucleon system. The calculations with Potential I on Bi^{210} showed that the central triplet-even part of the Potential I is somewhat too weak to account for the overall spacings of the multiplet $h_{9/2}\, g_{9/2}$. Hence, the central triplet-even strength was increased by a factor of about 1.6 in Potential II. The central triplet-odd part was neglected entirely in Potential II, because it was very small compared to the other components and did not affect the results very much. The singlet-odd force is repulsive, and it affects mostly the higher J states, particularly the J=9 state, as can be seen from the fig. 3. The central singlet-odd force of the Potential I was found to have an effect too strong for the J=9 level, thus bringing the latter level above the J=2 and 3 states in energy spectrum, and we arbitrarily reduced the strength of the central singlet-odd force by a factor of about three in the Potential II to bring the J=9 level down near the J=2 level. In the next calculation with the above modifications to the central force and somewhat strengthened tensor force, it was found that the positions of the 0- and 1- level were incorrect. Therefore, they were further strengthened to give the Potential II.

In fig. 8 and 9, we plot the effects on the ground-state multiplets of Bi^{210} and Po^{210} of adding successive components of our residual force.

The $h_{9/2}\, d_{5/2}$ and $h_{9/2}\, s_{1/2}$ multiplets of Bi^{210} seen in the (d,p) reaction are also plotted in fig. 8, and the $h_{9/2}\, i_{13/2}$ (J=4-, 5-) multiplet of Po^{210} is plotted in fig. 9. All diagonal matrix elements include central and tensor forces. In diagonalizing the matrix, only central-force contributions to the off-diagonal matrix elements were used in Po^{210}. For Bi^{210} the off-diagonal tensor-force matrix elements of the lowest three configurations $h_{9/2}\, g_{9/2}$, $h_{9/2}\, i_{11/2}$, and $f_{7/2}\, g_{9/2}$ were calculated and included, but only central-force off-diagonal elements apply to other configurations. A complete list of the eigenvalues for our calculations is presented in tables 3 and 4. The eigenfunctions are also calculated both for Bi^{210} and Po^{210} and are presented in tables 5 and 6, respectively. For Bi^{210}, the eigenfunctions are listed for the eigenvalues that correspond to the states arising from the lowest six odd-parity configurations, and for Po^{210} the eigenfunctions only for the even parity states are listed.

5. Discussion

From the analysis of various shell-model calculations and the study of the properties of nuclear matter, there are indications that the nuclear force inside the nucleus is not very different from the free two-nucleon force. We have relied upon the free two-nucleon potential in estimating the parameters of the central and tensor forces. Our analysis of the tensor-force effect indicates that the tensor force behaves quite differently from the central force and, indeed, seems to correct the order and spacing of the troublesome spin-0 and 1 levels in Bi^{210}. The analysis of Bi^{210} leads to the conclusion that the range of the tensor force in the residual interaction is about 2 fm or less. As shown clearly in figures 4 and 5, the infinite-range approximation for the tensor force is very dangerous. At the short ranges employed, the tensor force acts so specifically on two levels of spin 0 and 1 that it can not be simulated by a linear combination of the four central-force components. Our choice of the residual force which is slightly modified from the simulated BGT potential (Potential I) seems to give a rather good agreement with the experimental spectra. Since our residual force explains the ground-state multiplet of Bi^{210} very well, it is interesting to see if we can explain the other observed multiplets from our theoretical calculation. Levels from 0 to 0.581 MeV are clearly from the configuration $(h_{9/2}\ g_{9/2})$, and the spin assignments shown in fig. 8 are probably correct. Also the assignments of $(h_{9/2}\ d_{5/2})^{J=2}$ and $(h_{9/2}\ s_{1/2})^{J=4,5}$ for levels at 1.577, 2.517, and 2.572 MeV seem reasonable. Erskine suggested from the central-force calculation that levels at 0.672 and 0.912 are $(g_{9/2}\ i_{11/2})^{J=10}$ and $(f_{7/2}\ g_{9/2})^{J=8}$, respectively[5]. The relative cross sections also appear to support these assignments. Erskine et al. found that the level at 0.672 MeV is very weak, suggesting $(h_{9/2}\ i_{11/2})^{J=10}$.

If this is true, the other J states from $(h_{9/2}\ i_{11/2})$ are not expected to appear. Six levels ranging from 0.912 to 1.517 MeV are probably from the admixture of $(f_{7/2}\ g_{9/2})$ and $(h_{9/2}\ i_{11/2})$, the dominant part being $(f_{7/2}\ g_{9/2})$. Because of the configuration mixing, the relative cross sections are not very useful for assigning the spins for these levels. At higher energies, the various other factors such as core excitation and core vibration must be considered, and it is very difficult to conclude any assignments of spin and parity. However, six levels at 1.577, 1.916, 2.075, 2.138, 2.173, and 2.235 MeV have relatively smaller relative cross section than four levels at 1.972 (doublet), 2.027, and 2.102 MeV, and this suggests these six levels are probably from the admixture of $(h_{9/2}\ d_{5/2})$ and $(f_{7/2}\ i_{11/2})$, with $(h_{9/2}\ d_{5/2})$ being the dominant configuration. Four other levels at 1.972 (doublet), 2.027, and 2.102 MeV seem to come from the configuration $(p_{3/2}\ g_{9/2})$ arising from the core-excitation. It appears to be very difficult to assign configurations to the levels above 2.5 MeV, because the core vibration and core excitation become more important. The suggested spin and parity assignments for the levels below 2.6 MeV are summarized in table 7.

The β-decay properties of Bi^{210} have played an important role in the development of β-decay theory, because it is one of the few known cases of a first-forbidden transition $\Delta I = 1$(yes) showing striking deviations from the allowed shape. The so-called ξ approximation can explain the spectrum shape if certain beta-decay matrix elements bear certain ratios to each other. As an independent check from the shell-model theory on the value of ξ, which is the ratio $i\langle \underset{\sim}{r} \rangle / \langle \underset{\sim}{\sigma} \times \underset{\sim}{r} \rangle$, we present the value of ξ that is consistent with our level-scheme calculation. Using the ground-state wave functions presented in tables 5 and 6, we find $\xi \approx -0.63$. (Only the lowest three configurations are used for Bi^{210}.) For the pure configuration $h_{9/2}\ i_{11/2}$,

the value of ξ is +1.0, whereas it is -0.1 for the pure $h_{9/2}\ g_{9/2}$ configuration[1]. The recent paper by Fujita[14] on the beta-decay of RaE based upon the conserved-current hypothesis of Feynman and Gell-Man[15] indicated that the value of ξ should be $-1.2 \leqslant \xi \leqslant -0.48$ in order to fit both the beta-spectrum shape and the beta-polarization data, whereas we have $-1.2 \leqslant \xi \leqslant 0.12$ if we consider only the spectrum shape. Our value of $\xi = -0.63$ is consistent with the limit set by Fujita.

The reason we obtain the value of $\xi(-0.63)$ outside the limit of two extreme pure configuration ($\xi = -0.1$ for $h_{9/2}\ g_{9/2}$ and $\xi = 1.0$ for $h_{9/2}\ i_{11/2}$) is the large positive value of the off-diagonal tensor-force matrix element $\langle h_{9/2}\ g_{9/2}|V^T(\underset{\sim}{r}_{12})S_{12}|h_{9/2}\ i_{11/2}\rangle$, which in turn yields a negative component of the eigenvector $|h_{9/2}\ i_{11/2}\rangle$. To show that the off-diagonal tensor-force matrix element $\langle h_{9/2}\ g_{9/2}|V^T(\underset{\sim}{r}_{12})S_{12}|h_{9/2}\ i_{11/2}\rangle$ is positive and rather large for the range we are using, we plot $(1/3)\langle h_{9/2}\ g_{9/2}|P_{TE}\ U_{TE}{}^T\ (\underset{\sim}{r}_{12})\ S_{12}|\ h_{9/2}\ i_{11/2}\rangle$ and $(1/3)\langle h_{9/2}\ g_{9/2}|P_{TO}\ U_{TO}{}^T(\underset{\sim}{r}_{12})\ S_{12}|h_{9/2}\ i_{11/2}\rangle$ as a function of the force range in fig. 10. The central-force off-diagonal matrix element is smaller and of the opposite sign compared to the tensor, so we see the essential role of the tensor force in inducing configuration mixtures of the proper phase to explain the beta-decay phenomena.

Most recently, a reanalysis by Spector[16] of RaE beta decay has established the limits $-1.6 < \xi < -0.8$, which largely overlap Fujita's limits. From a shell-model analysis in which the mixing of the core-excited states is taken into account through the delta-function force, Spector obtains $\xi \approx -1$ for $\Delta E = \hbar\omega \approx 4$ MeV. The strength of the delta-function force is chosen by Spector so as to preserve the volume energy of the delta-function potential when compared to the finite-range force used by Newby and Konopinski[1]. Therefore, we feel that Spector's calculation may overestimate

the amplitudes of mixing of the core-excited states, because it is known[17,18] that this choice of the strength of the delta-function force yields larger matrix elements (by a factor of 3 to 4) than the finite-range force used by Newby and Konopinski. We feel that the dominant consideration leading to satisfactory ξ values for the shell model is the reversed sign of the configuration mixture of the principal two configurations, as caused by the tensor force. The additional smaller contribution due to the core-excited states may well bring our value of ξ (= -0.63) within the limit ($-1.6 < \xi < -0.8$) set by Spector. More refined analysis is necessary to obtain quantitative results with inclusion of both the core excitation and the tensor force.

Another interesting quantity is the magnetic dipole moment of Bi^{210}. Using the atomic-beam technique, Alpert et al. have measured this moment to be 0.0442±0.0001 nm[19]. If one assumes pure configurations, the magnetic moment in the Schmidt limit is +0.08 nm for $h_{9/2}\ g_{9/2}$, -0.36 nm for $h_{9/2}\ i_{11/2}$, and -4.07 nm for $f_{7/2}\ g_{9/2}$. On the other hand, if you use the empirical g factor for the $h_{9/2}$ proton from Bi^{209} (unfortunately the empirical g factor for the $g_{9/2}$ neutron is not known yet), the magnetic moment of Bi^{210} is 0.24 nm and -1.08 nm for the pure configuration of $h_{9/2}\ g_{9/2}$ and $h_{9/2}\ i_{11/2}$ respectively.

Using our wave function for the 1- state of Bi^{210},

$$\psi_{Bi^{210}}(J=1) = 0.9767|h_{9/2}\ g_{9/2}\rangle - 0.1883\ |h_{9/2}\ i_{11/2}\rangle + 0.0578\ |f_{7/2}\ g_{9/2}\rangle,$$

we find the magnetic dipole moment of Bi^{210} to be 0.050 nm in the Schmidt limit, whereas it is 0.177 nm if we take the empirical g factor for the $h_{9/2}$ proton. Because the measured magnetic moment is small and the sign of the moment is not determined by the experiment, the above calculated results seem to be consistent with the experiment. It should be noted that the wave function of the Bi^{210} ground state obtained by Newby and Konopinski yields

the magnetic moment of -0.75 nm.

For Po^{210}, we note at 2.91 MeV a predicted state $(h_{9/2}\ i_{13/2})^{J=11-}$ which could be an isomeric state of detectable half life. It cannot decay by dipole or quadrupole transitions but may decay into the state $(h_{9/2}\ h_{9/2})^{J=8+}$ (1.57 MeV) or $(h_{9/2}\ f_{7/2})^{J=8+}$ (2.46 MeV) by E3 transitions, which then may cascade to the ground state by several E2 transitions. This is schematically shown in fig. 11. Calculations with our eigenfunctions predict considerable retardation below single-particle strength for the higher energy E3. For the E3 transitions the product of the partial gamma half life and transition energy to the seventh power should be $t_{1/2}E^7 = 2.3 \times 10^{-5}$ sec MeV^7 for the 1.34-MeV E3 and $t^{1/2}E^7 = 7.5 \times 10^{-6}$ sec MeV^7 for the 0.45-MeV transition. The half life of the 11- state should be a few microseconds. (Here we have used the harmonic-oscillator radial wave functions, and an effective charge of 1.0e is assumed.)

Funk et al.[20] have recently measured the γ-transition probabilities of 46.7 keV(6+ ⟶ 4+) and 246 keV(4+ ⟶ 2+) in Po^{210}. They obtained 5.3×10^{4} sec^{-1} and 3.1×10^{8} sec^{-1}, respectively. Our eigenfunctions for the lowest 2+, 4+, and 6+ states show so little configuration mixing that it is appropriate to calculate the shell-model lifetimes between pure $(h_{9/2})^2_J$ states and estimate an effective charge for the protons. We have computed these E2 transition probabilities, using our wave functions presented in table 5 with the harmonic radial wave functions. The effect of configuration mixing was found to be negligible, and the ratio of the observed to calculated transition probabilities is $T(E3)_{obs}/T(E3)_{calc} = 8.2$ for both 46.7-keV and 246-keV transitions. One may attempt to explain this discrepancy by assuming the effective charge of $(8.2e)^{1/2}$ ($\cong 2.86e$) for the proton. The presence of the extra protons outside the core tends to polarize the core, thus giving rise

to the effective increase of the proton charge. The effective proton charge due to the polarized core is expected to be

$$e_{eff.} = e(1 + \frac{Z}{A}\gamma),$$

where γ is 1 for the harmonic-oscillator potential[21] and γ is 3 to 5 for the square-well potential[22]. Our value of $\gamma = 2.15$ seems reasonable if one notes that various effects such as the core excitation and vibration have not been taken into account in our calculation.

The residual force (Potential I) presented in table 2 was also used in the calculation of the low-energy spectrum of the odd-odd nucleus Y^{90}. For this nucleus the central force with a reasonable singlet-even to triplet-even ratio of ~ 0.5 does not yield the experimental sequence of the observed levels[9]. However, inclusion of the tensor force in our residual force eliminated this difficulty, giving rise to a rather good agreement with the experimental spectrum of Y^{90}.

The tensor force has been neglected in most of the past shell-model calculations primarily because of the computational complexity involved, but with the hope that the tensor-force effects are small and may be simulated by an effective central force. That this not always true is clearly shown in our calculations on Bi^{210}. The general success of past central-force calculations may be due to the tensor-force matrix elements being small in most cases. However, we see here that configurations of high j with parallel or antiparallel alighment of angular momenta can experience appreciable tensor-force effects. Furthermore, inclusion of the tensor force may lead us to a better understanding of the residual force in the nucleus, and we may hope to find a residual force that can be used without alteration for different nuclei.

Acknowledgments

We would like to express our gratitude to Dr. John R. Erskine for providing the experimental information on Bi^{210} prior to publication. Discussions with Dr. Hans J. Mang were very helpful. The computational work was carried out on the IBM-7090 computer at this Laboratory.

REFERENCES

1) M. H. L. Price, Proc. Phys. Soc. (London) A65 (1952) 773;N. Newby and E. J. Konopinski, Phys. Rev. 115 (1959) 434; J. Flores and P. A. Mello, Bull. Am. Phys. Soc. 8 (1963) 129, Abstract W5

2) Yu. I. Kharitonov, L. A. Sliv, and G. A. Sogomonova, Nuclear Physics 28 (1961) 210

3) A. de-Shalit and J. D. Walecka, Nuclear Physics 22 (1961) 184

4) J. R. Erskine, W. W. Buechner, and H. A. Enge, Phys. Rev. 128 (1962) 720

5) J. R. Erskine, Massachusetts Institute of Technology, private communication

6) R. W. Hoff and J. M. Hollander, Phys. Rev. 109 (1958) 447

7) P. Mukherjee and B. L. Cohen, Phys. Rev. 127 (1962) 1284

8) I. Talmi, Phys. Rev. 89 (1953) 1065

9) Y. E. Kim, Lawrence Radiation Laboratory Report UCRL-10329, February 22, 1963, submitted to Phys. Rev.

10) J. F. Dawson, I. Talmi, and J. D. Walecka, Ann. of Phys. (N. Y.) 18 (1962) 339

11) K. A. Brueckner and J. L. Gammel, Phys. Rev. 109 (1958) 1023

12) J. M. Blatt and J. D. Jackson, Phys. Rev. 76, (1949) 18

13) M. H. Kalos, L. C. Biedenharn, and J. M. Blatt, Nuclear Physics 1 (1956) 233

14) Jun-Ichi Fujita, Phys. Rev. 126 (1962) 202

15) R. Feynman and M. Gell-Mann, Phys. Rev. 109 (1958) 193

16) R. M. Spector, Nuclear Physics 40 (1963) 338

17) H. J. Mang, Lawrence Radiation Laboratory, private communication

18) M. Redlich, Lawrence Radiation Laboratory, private communication

19) S. S. Alpert, E. Lipworth, M. B. White, and K. F. Smith, Phys. Rev. 125 (1962) 256

20) E. G. Funk, Jr., H. J. Prask, F. Schima, J. McNulty, and J. W. Mihelich, Phys. Rev. 129 (1962) 757

REFERENCES (continued)

21) B. Mottelson, Nordita Publ. No. 20 (1959), Cours de l'Ecole d'Eté de Physique Théorique des Houches (Dunod, Paris, 1959)

22) Z. Szymanski, Bull. Acad. Pol. Sci., Ser. des Sci. math. astr. et phys. 7 (1959) 233

FOOTNOTE

† This work was done under the auspices of the U. S. Atomic Energy Commission.

Table 1

Independent-particle energies[a] for Bi^{210} and Po^{210}

Bi^{210}		Po^{210}	
Configuration (proton-neutron)	Energy (MeV)	Configuration (proton-proton)	Energy (MeV)
$h_{9/2}\ g_{9/2}$	0.0	$h_{9/2}\ h_{9/2}$	0.0
$h_{9/2}\ i_{11/2}$	0.77	$h_{9/2}\ f_{7/2}$	0.90
$f_{7/2}\ g_{9/2}$	0.90	$h_{9/2}\ i_{13/2}$	1.62
$h_{9/2}\ j_{15/2}$	1.41	$f_{7/2}\ f_{7/2}$	1.80
$h_{9/2}\ d_{5/2}$	1.56	$f_{7/2}\ i_{13/2}$	2.52
$f_{7/2}\ i_{11/2}$	1.67	$i_{13/2}\ i_{13/2}$	3.24
$h_{9/2}\ s_{1/2}$	2.03		
$f_{7/2}\ j_{15/2}$	2.31		
$f_{7/2}\ d_{5/2}$	2.46		
$h_{9/2}\ g_{7/2}$	2.47		
$h_{9/2}\ d_{3/2}$	2.52		
$f_{7/2}\ s_{1/2}$	2.93		
$f_{7/2}\ g_{7/2}$	3.37		
$f_{7/2}\ d_{3/2}$	3.42		

a) The single-particle energies are taken from references 6 and 7.

Table 2

Values of the force parameters for the BGT potential, the simulated Gaussian potential (Potential I), and the adjusted potential used in this paper (Potential II).

Force components	BGT Potential		Potential I		Potential II	
	Strength (MeV)	Range (fm)	Strength (MeV)	Range (fm)	Strength (MeV)	Range (fm)
Central triplet-even	-877.39	0.478	-223.02	0.706	-355.24	0.706
Central singlet-even	-434.0	0.690	-110.03	1.018	-133.20	1.018
Central triplet-odd	- 14.0	1.00	- 3.57	1.476	0.0	-----
Central singlet-odd	130.0	1.00	33.06	1.476	11.01	1.476
Tensor triplet-even	-159.40	0.953	- 40.50	1.407	- 99.28	1.407
Tensor triplet-odd	22.0	1.25	5.58	1.845	9.50	1.845

Table 3

Calculated eigenvalues and energy levels in Bi^{210}. In the last column, eigenvalues are expressed in a new energy scale in which the ground state lies at zero energy. The indicated configuration is taken to be the dominant one.

Configuration (proton-neutron)	Jπ	Eigenvalues (MeV)	Energy (MeV)
$h_{9/2}\ g_{9/2}$	0-	-0.572	0.022
	1-	-0.594	0.0
	2-	-0.311	0.283
	3-	-0.251	0.343
	4-	-0.135	0.459
	5-	-0.202	0.392
	6-	-0.084	0.510
	7-	-0.218	0.376
	8-	-0.062	0.532
	9-	-0.310	0.284
$h_{9/2}\ i_{11/2}$	1-	0.076	0.670
	2-	0.534	1.128
	3-	0.573	1.167
	4-	0.688	1.282
	5-	0.655	1.249
	6-	0.646	1.240
	7-	0.708	1.302
	8-	0.345	0.939
	9-	0.753	1.347
	10-	0.212	0.806
$f_{7/2}\ g_{9/2}$	1-	0.529	1.123
	2-	0.701	1.295
	3-	0.796	1.390
	4-	0.776	1.370
	5-	0.818	1.412
	6-	0.761	1.355
	7-	0.854	1.448
	8-	0.671	1.265
$h_{9/2}\ d_{5/2}$	2-	1.015	1.609
	3-	1.390	1.984
	4-	1.390	1.984
	5-	1.421	2.015
	6-	1.483	2.077
	7-	1.402	1.996

Table 3 (continued)

Configuration (proton-neutron)	Jπ	Eigenvalues (MeV)	Energy (MeV)
$f_{7/2}\ i_{11/2}$	2-	1.358	1.952
	3-	1.469	2.063
	4-	1.529	2.123
	5-	1.498	2.092
	6-	1.573	2.167
	7-	1.490	2.084
	8-	1.600	2.194
	9-	1.324	1.918
$h_{9/2}\ s_{1/2}$	4-	1.869	2.463
	5-	1.970	2.564
$f_{7/2}\ d_{5/2}$	1-	2.066	2.660
	2-	2.256	2.850
	3-	2.283	2.877
	4-	2.263	2.857
	5-	2.393	2.987
	6-	2.126	2.720
$h_{9/2}\ g_{7/2}$	1-	2.176	2.770
	2-	2.444	3.038
	3-	2.354	2.948
	4-	2.390	2.984
	5-	2.417	3.011
	6-	2.235	2.829
	7-	2.449	3.043
	8-	2.180	2.774
$h_{9/2}\ d_{3/2}$	3-	2.485	3.079
	4-	2.521	3.115
	5-	2.505	3.099
	6-	2.476	3.070
$f_{7/2}\ s_{1/2}$	3-	2.800	3.394
	4-	2.778	3.372
$f_{7/2}\ g_{7/2}$	0-	2.530	3.124
	1-	2.698	3.292
	2-	3.034	3.628
	3-	3.035	3.629
	4-	3.220	3.814
	5-	3.056	3.650
	6-	3.268	3.862
	7-	2.942	3.536

Table 3 (continued)

Configuration (proton-neutron)	Jπ	Eigenvalues (MeV)	Energy (MeV)
$f_{7/2}\ d_{3/2}$	2-	3.094	3.688
	3-	3.247	3.841
	4-	3.327	3.921
	5-	3.156	3.750
$h_{9/2}\ j_{15/2}$	3+	0.496	1.090
	4+	1.083	1.677
	5+	1.140	1.734
	6+	1.131	1.725
	7+	1.249	1.846
	8+	1.133	1.727
	9+	1.290	1.884
	10+	1.090	1.684
	11+	1.311	1.905
	12+	0.880	1.474
$f_{9/2}\ j_{15/2}$	4+	2.051	2.645
	5+	2.243	2.837
	6+	2.230	2.824
	7+	2.221	2.815
	8+	2.269	2.863
	9+	2.177	2.771
	10+	2.291	2.885
	11+	1.969	2.563

Table 4

Calculated eigenvalues and energy levels in Po^{210}. In the last column, eigenvalues are expressed in a new energy scale in which the ground state lies at zero energy. The indicated configuration is taken to be the dominant one.

Configuration (proton-proton)	$J\pi$	Eigenvalues (MeV)	Energy (MeV)
$h_{9/2}\ h_{9/2}$	0+	-1.597	0.0
	2+	-0.373	1.224
	4+	-0.166	1.431
	6+	-0.084	1.513
	8+	-0.027	1.570
$h_{9/2}\ f_{7/2}$	1+	0.303	1.900
	2+	0.582	2.179
	3+	0.792	2.389
	4+	0.928	2.525
	5+	0.855	2.452
	6+	0.896	2.493
	7+	0.864	2.461
	8+	0.863	2.460
$f_{7/2}\ f_{7/2}$	0+	0.868	2.465
	2+	0.764	2.361
	4+	1.664	3.261
	6+	1.741	3.338
$i_{13/2}\ i_{13/2}$	0+	2.718	4.315
	2+	2.903	4.500
	4+	3.050	4.647
	6+	3.118	4.715
	8+	3.158	4.755
	10+	3.187	4.784
	12+	3.222	4.819
$h_{9/2}\ i_{13/2}$	2-	1.526	3.123
	3-	1.645	3.242
	4-	1.575	3.172
	5-	1.602	3.199
	6-	1.582	3.179
	7-	1.567	3.164
	8-	1.583	3.180
	9-	1.510	3.107
	10-	1.583	3.180
	11-	1.315	2.912
$f_{7/2}\ i_{13/2}$	3-	2.315	3.912
	4-	2.497	4.094
	5-	2.438	4.035
	6-	2.510	4.107
	7-	2.474	4.071
	8-	2.512	4.109
	9-	2.499	4.096
	10-	2.506	4.103

Table 5.

Calculated eigenfunctions for Bi^{210}.

Eigenvalues (MeV)	Eigenfunctions											
	$h_{9/2}\,g_{9/2}$	$h_{9/2}\,i_{11/2}$	$f_{7/2}\,g_{9/2}$	$h_{9/2}\,d_{5/2}$	$f_{7/2}\,i_{11/2}$	$h_{9/2}\,s_{1/2}$	$f_{7/2}\,d_{5/2}$	$h_{9/2}\,g_{7/2}$	$h_{9/2}\,d_{3/2}$	$f_{7/2}\,s_{1/2}$	$f_{7/2}\,g_{7/2}$	$f_{7/2}\,d_{3/2}$
J = 0												
-0.572	-0.9999										0.0099	
J = 1												
-0.594	0.9767	-0.1883	0.0578				0.0130	-0.0819			-0.0130	
0.076	0.0893	0.6836	0.7167				0.0753	0.0232			-0.0686	
0.529	0.1735	0.6925	-0.6708				0.0680	-0.0154			0.1878	
J = 2												
-0.311	-0.9727	-0.1114	0.0175	-0.1049	0.1696		-0.0010	-0.0305			0.0073	0.0139
0.534	-0.1694	0.9000	-0.1774	0.0038	-0.3500		-0.0480	0.0638			-0.0131	0.0233
0.701	-0.0094	-0.2073	-0.9711	0.1073	-0.0300		-0.0272	0.0017			0.0114	0.0211
1.015	-0.1564	-0.2632	0.1510	0.6690	-0.6403		-0.0089	0.1526			-0.0458	-0.0153
1.358	-0.0065	-0.2511	-0.0063	-0.7205	-0.6459		0.0030	0.0141			0.0015	-0.0123
J = 3												
-0.251	-0.9951	0.0212	-0.0151	-0.0593	-0.0660		-0.0053	0.0041	0.0272	-0.0136	-0.0006	-0.0088
0.573	-0.0145	-0.8796	-0.4721	0.0186	0.0230		-0.0277	-0.0193	-0.0125	-0.0116	0.0286	0.0057
0.796	-0.0187	-0.4734	0.8758	0.0121	-0.0586		0.0021	-0.0002	0.0447	-0.0058	-0.0520	-0.0058
1.390	-0.0909	0.0140	0.0441	0.7650	0.6245		0.0031	-0.0543	-0.0957	0.0138	0.0368	0.0213
1.469	-0.0132	-0.0181	0.0514	-0.6366	0.7657		-0.0187	-0.0641	-0.0158	-0.0048	0.0092	0.0173
J = 4												
-0.135	0.9944	0.0643	0.0168	0.0407	-0.0606	0.0227	0.0100	0.0160	0.0124	0.0122	-0.0071	-0.0078
0.688	-0.0691	0.9414	0.3117	-0.0259	-0.0858	-0.0493	-0.0129	0.0196	-0.0221	-0.0092	-0.0106	-0.0007
0.776	-0.0040	0.3112	-0.9492	-0.0003	-0.0311	0.0026	-0.0265	0.0073	0.0101	0.0025	0.0120	0.0110
1.390	-0.0702	-0.0154	0.0116	0.8492	-0.4537	0.2189	0.0040	0.0981	0.0953	0.0064	-0.0259	-0.0090
1.529	-0.0266	-0.0963	-0.0027	-0.4679	-0.8762	-0.0371	0.0085	0.0396	0.0035	0.0101	-0.0064	-0.0088
0.869	-0.0153	0.0446	0.0173	-0.2299	0.0829	0.9519	-0.0240	0.1039	0.1395	-0.0120	-0.0225	-0.0008

Table 5 (Continued)

Eigenvalues (MeV)	Eigenfunctions										
	$h_{9/2}g_{9/2}$	$h_{9/2}i_{11/2}$	$f_{7/2}g_{9/2}$	$h_{9/2}d_{5/2}$	$f_{7/2}i_{11/2}$	$h_{9/2}s_{1/2}$	$f_{7/2}d_{5/2}$	$h_{9/2}g_{7/2}$	$h_{9/2}d_{3/2}$	$f_{7/2}s_{1/2}$	$f_{7/2}g_{7/2}$	$f_{7/2}d_{3/2}$
J = 5												
-0.202	-0.9967	-0.0005	-0.0107	-0.0565	-0.0410	-0.0326	-0.0049	-0.0081	-0.0030		-0.0136	-0.0103
0.655	-0.0020	0.9564	0.2849	-0.0212	-0.0444	-0.0200	0.0134	0.0119	0.0001		-0.0258	-0.0107
0.818	-0.0106	-0.2857	0.9554	0.0353	-0.0291	0.0343	0.0041	0.0005	0.0175		-0.0419	-0.0022
1.421	-0.0715	0.0433	-0.0199	0.9421	0.2651	0.1841	0.0067	0.0027	-0.0156		0.0204	0.0103
1.498	-0.0198	0.0249	0.0498	-0.2624	0.9575	-0.0499	-0.0205	-0.0686	-0.0335		0.0248	0.0365
1.970	-0.0222	0.0219	-0.0213	-0.1952	0.0006	0.9788	0.0324	0.0339	0.0022		0.0111	-0.0027
J = 6												
-0.084	-0.9953	-0.0739	-0.0334	-0.0210	0.0348		-0.0091	-0.0197	-0.0229		0.0018	
0.646	-0.0809	0.8091	0.5785	-0.0069	-0.0516		0.0018	0.0149	-0.0272		-0.0164	
0.761	-0.0157	0.5786	-0.8142	-0.0139	-0.0251		-0.0277	0.0110	-0.0092		0.0118	
1.483	-0.0346	-0.0062	-0.0108	0.9381	-0.3194		0.0154	0.0743	0.1032		-0.0106	
1.573	-0.0226	-0.0594	-0.0079	-0.3297	-0.9392		0.0309	0.0546	0.0330		-0.0058	
J = 7												
-0.218	-0.9960	-0.0166	-0.0087	-0.0829	-0.0207			-0.0106			0.0012	
0.708	-0.0142	0.9827	0.1686	-0.0313	-0.0591			0.0072			-0.0331	
0.854	-0.0090	-0.1708	0.9819	0.0488	-0.0301			0.0004			-0.0569	
1.402	-0.0846	0.0416	-0.0404	0.9919	0.0707			0.0215			0.0045	
1.490	-0.0151	0.0513	0.0452	-0.0713	0.9924			-0.0572			0.0423	
J = 8												
-0.062	0.9884	0.1138	0.0928		-0.0204			0.0316				
0.345	0.1333	-0.4186	-0.8979		0.0249			-0.0075				
0.671	0.0648	-0.8991	0.4301		0.0383			-0.0280				
1.600	0.0176	0.0507	0.0074		0.9917			-0.1158				
J = 9												
-0.310	0.9993	0.0363			-0.0026							
0.753	0.0364	-0.9946			0.0962							
1.324	0.0008	-0.0963			-0.9953							

Table 6

Calculated eigenfunctions for the even-parity states in Po^{210}

Eigenvalue (MeV)	Eigenfunctions			
	$h_{9/2}\ h_{9/2}$	$h_{9/2}\ f_{7/2}$	$f_{7/2}\ f_{7/2}$	$i_{13/2}\ i_{13/2}$
J = 0				
-1.597	-0.8845		-0.3032	0.3544
1.016	-0.3697		0.9190	-0.1364
2.718	-0.2844		-0.2517	-0.9250
J = 2				
-0.372	-0.9895	-0.0305	-0.0873	0.1109
0.928	-0.0350	0.9989	0.0216	-0.0208
1.518	-0.0979	-0.0269	0.9896	-0.1013
2.904	-0.1003	-0.0217	-0.1116	-0.9884
J = 4				
-0.166	-0.9965	-0.0369	-0.0446	0.0589
0.896	-0.0390	0.9988	0.0152	-0.0224
1.664	-0.0474	-0.0183	0.9969	-0.0586
3.051	-0.0553	-0.0236	-0.0616	-0.9962
J = 6				
-0.084	-0.9980	-0.0433	-0.0254	-0.0383
0.0863	-0.0446	0.9986	0.0113	-0.0251
1.741	-0.0263	-0.0134	0.9989	-0.0363
3.118	-0.0362	-0.0263	-0.0376	-0.9982
J = 8				
-0.027	-0.9977	-0.0622		0.0260
0.764	-0.0630	0.9974		-0.0336
3.158	-0.0239	-0.0352		-0.9900

Table 7

Suggested spin and parity assignments for levels below 2.6 MeV in Bi^{210}. Level energies and relative differential cross sections are taken from Erskine et al. (reference 3). The spins for $(h_{9/2}\ g_{9/2})^{J=0,\ldots,9}$, $(h_{9/2}\ d_{5/2})^{J=2}$, and $(h_{9/2}\ s_{1/2})^{J=4,5}$ have been suggested by Erskine et al.

Energy (MeV)	Relative differential cross section	Suggested Jπ	Suggested configuration
0.0	1.4	1-	$(h_{9/2}\ g_{9/2})$
0.047	0.4	0-	
0.268	9.6	9-	
0.320	2.3	2-	
0.347	3.8	3-	
0.433	14.9	5- and 7-	
0.501	5.3	4-	
0.547	7.0	6-	
0.581	8.0	8-	
0.672	0.4	(10-)	$(h_{9/2}\ i_{11/2})$
0.912	1.9	(8-)	$\alpha(f_{7/2}\ g_{9/2})+\beta(h_{9/2}\ i_{11/2})$
1.172	1.2	(3- or 5-)	
1.325	0.9	(5- or 3-)	
1.372	1.0	(4-)	
1.460	1.6	(6- or 7-)	
1.517	1.4	(7- or 6-)	
1.577	6.9	2-	$\gamma(h_{9/2}d_{5/2})+\delta(f_{7/2}\ i_{11/2})$
1.916	21.6	(4-)	
2.075	26.3	(7-)	
2.138	9.3	(3-)	
2.173	24.9	(6-)	
2.235	23.5	(5-)	
1.972 (doublet)	123	(3- and 6-)	$(p_{3/2}\ g_{9/2})$
2.027	58.9	(5-)	
2.102	51.4	(4-)	
2.517	125	4-	$(h_{9/2}\ s_{1/2})$
2.572	181	5-	

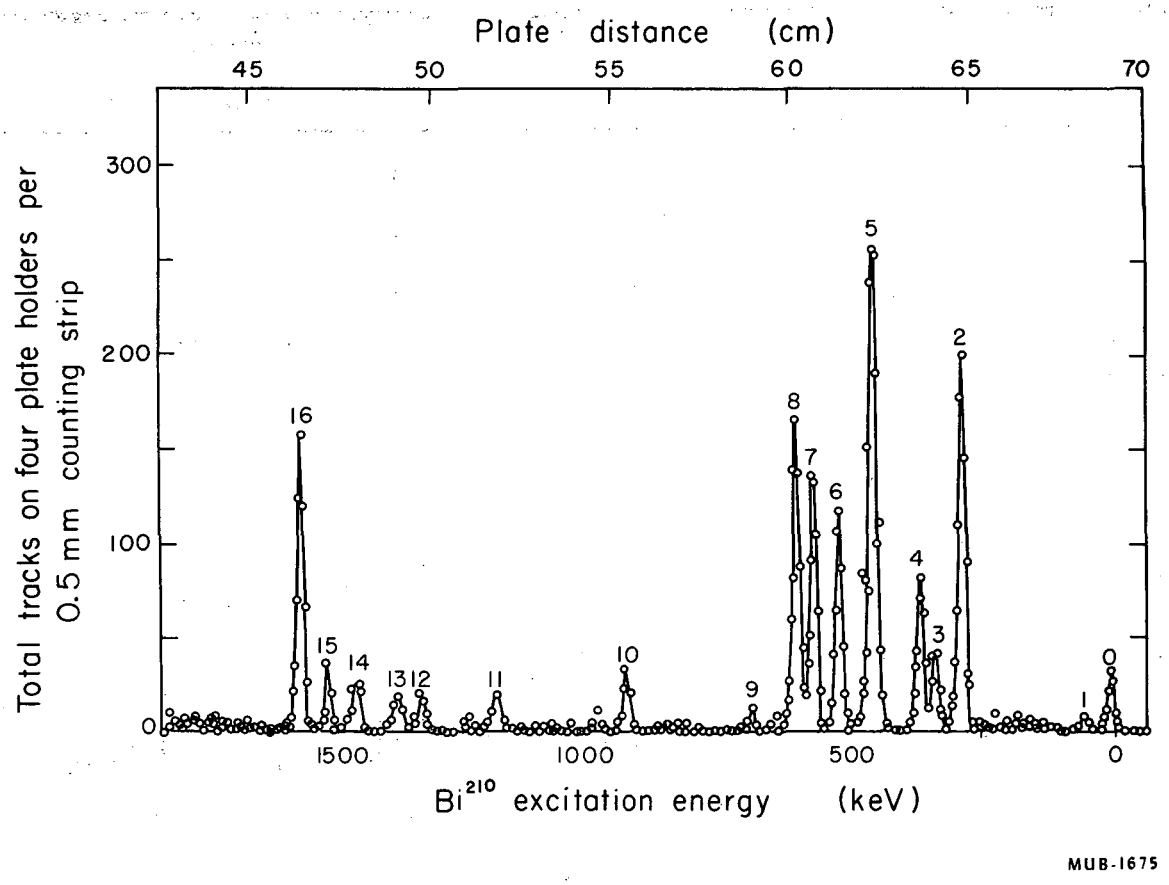

Fig. 1. Spectrum of protons from (d,p) reaction on Bi^{209} as observed by Erskine et al. (ref. 3).

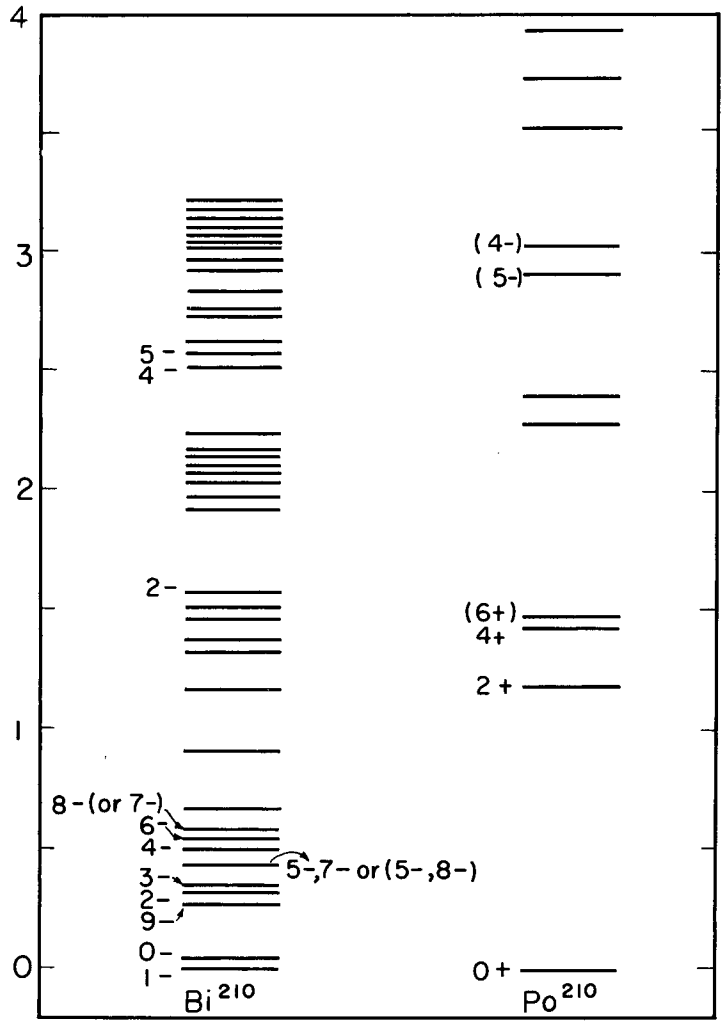

Fig. 2. The experimentally observed low-lying energy levels in Bi^{210} and Po^{210}.

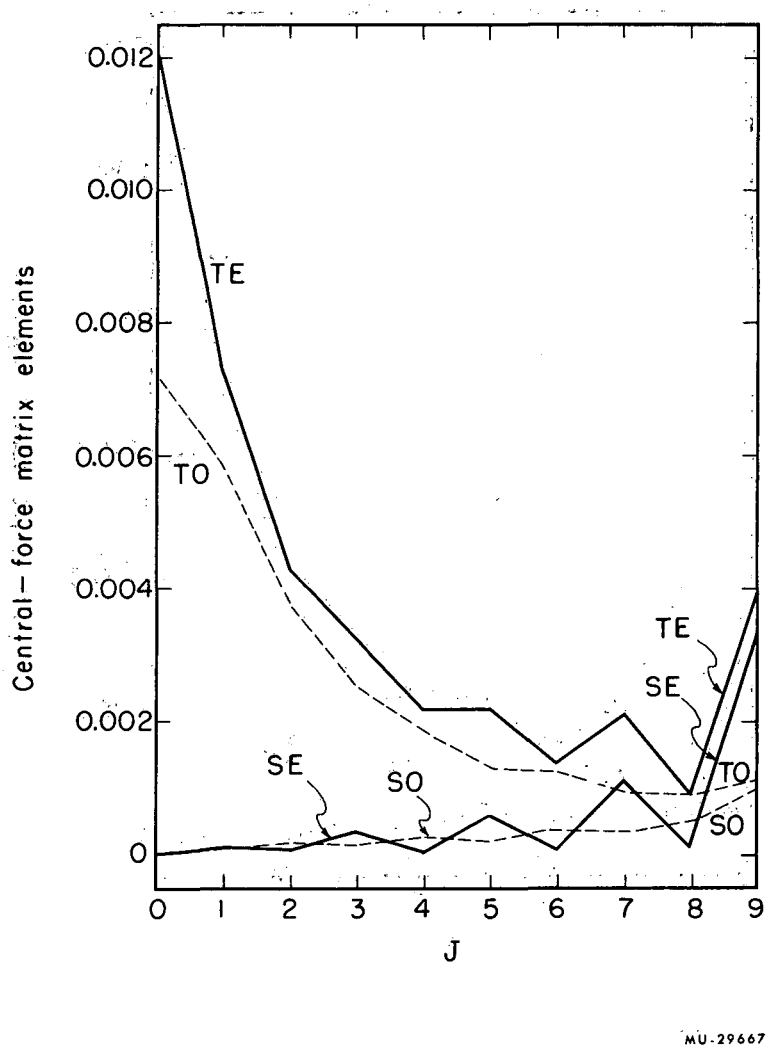

Fig. 3. The matrix elements of the four central-force components for the configuration $h_{9/2}\, g_{9/2}$ in Bi^{210}. The same range 1.5 fm is taken for all cases. The symbols TE, SE, TO, and SO stand for triplet-even, singlet-even, triplet-odd, and singlet-odd, respectively.

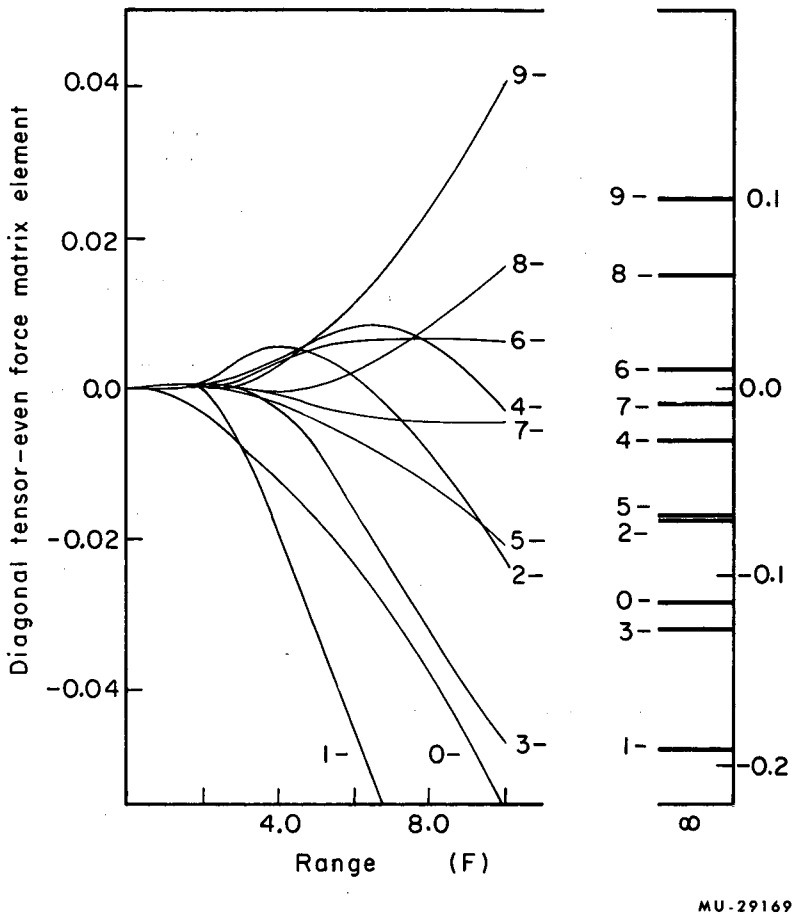

Fig. 4. Diagonal matrix elements of the tensor-even force $(1/3)P_{TE}\, U^{T}_{TE}(r_{12})S_{12}$ for the multiplet $h_{9/2}\, g_{9/2}$ in Bi^{210} as a function of the range parameter $(\beta^{T}_{TE})^{-1/2}$.

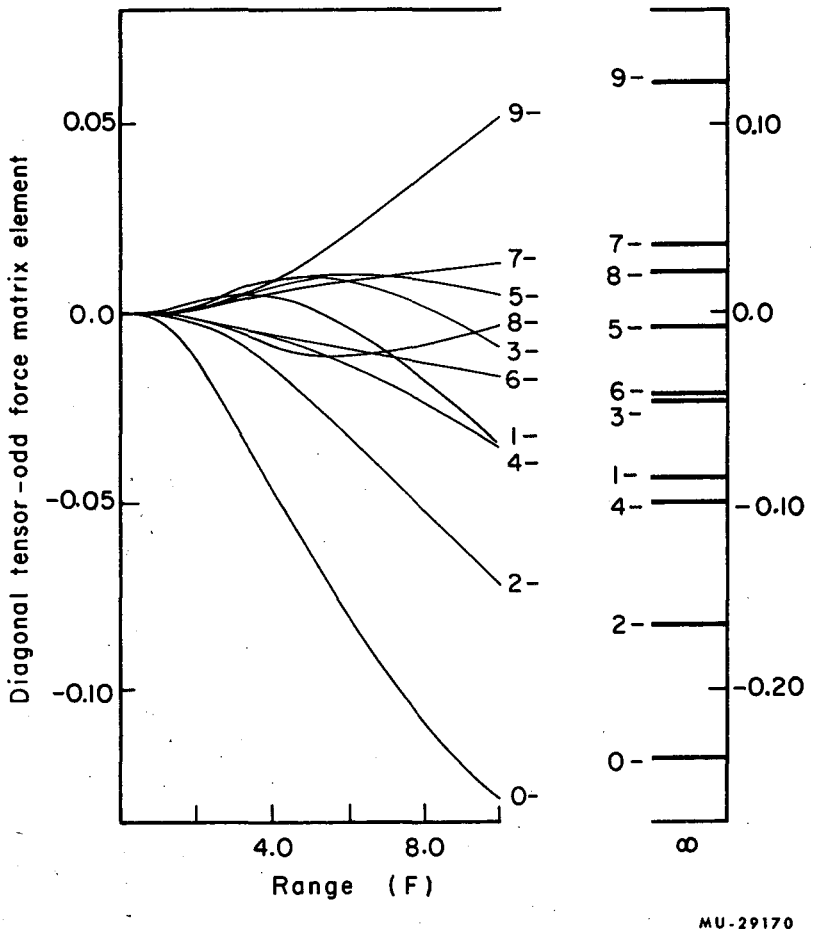

Fig. 5. Diagonal matrix elements of the tensor-odd force $(1/3)P_{TO}\ U^{T}_{TO}(r_{12})S_{12}$ for the multiplet $h_{9/2}\ g_{9/2}$ in Bi^{210} as a function of the range parameter $(\beta^{T}_{TO})^{-1/2}$.

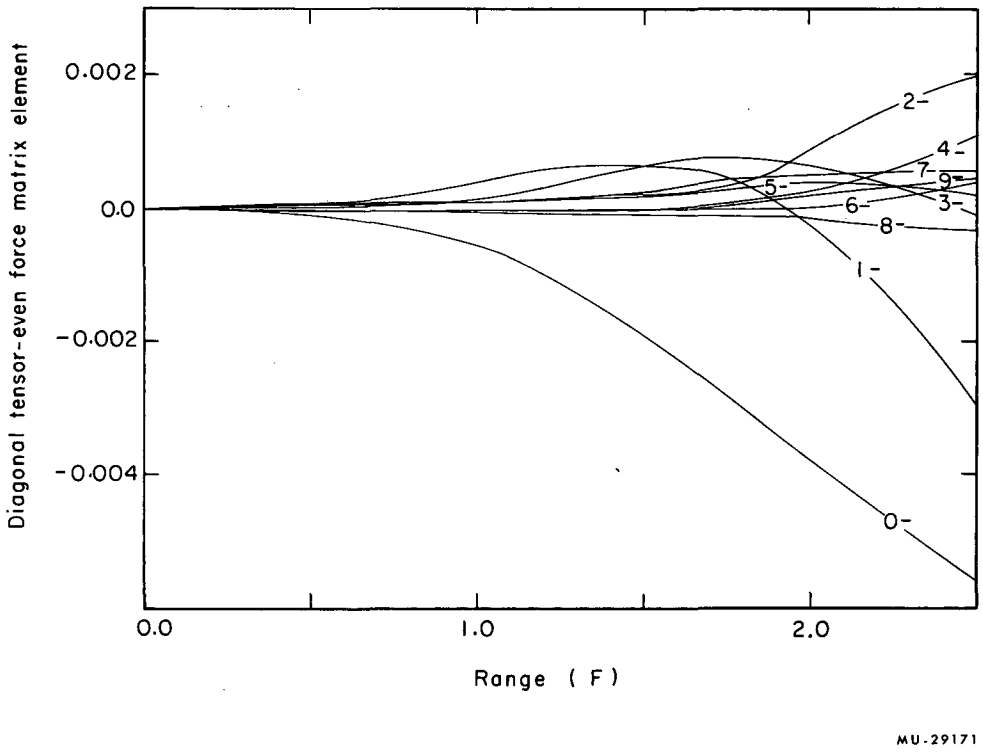

Fig. 6. Diagonal matrix elements of the tensor-even force for the multiplet $h_{9/2}\ g_{9/2}$ in Bi^{210} as a function of the range at the shorter ranges.

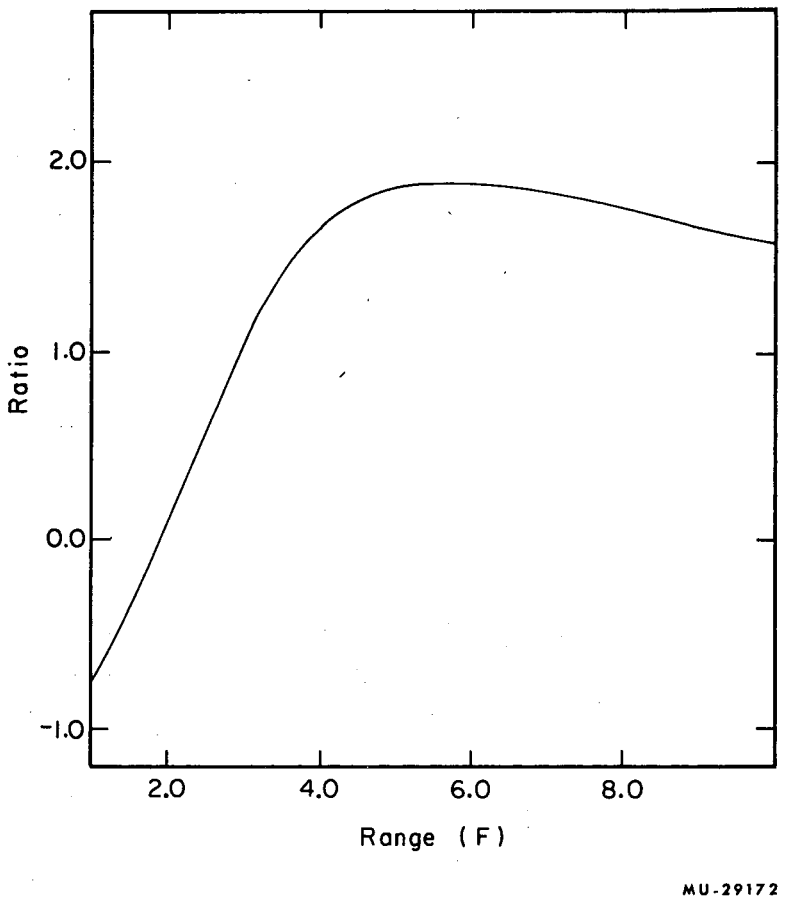

Fig. 7. Ratio of the diagonal tensor-even force matrix element for the spin-1 state to the spin-0 state of the configuration $h_{9/2}\, g_{9/2}$ as a function of the range.

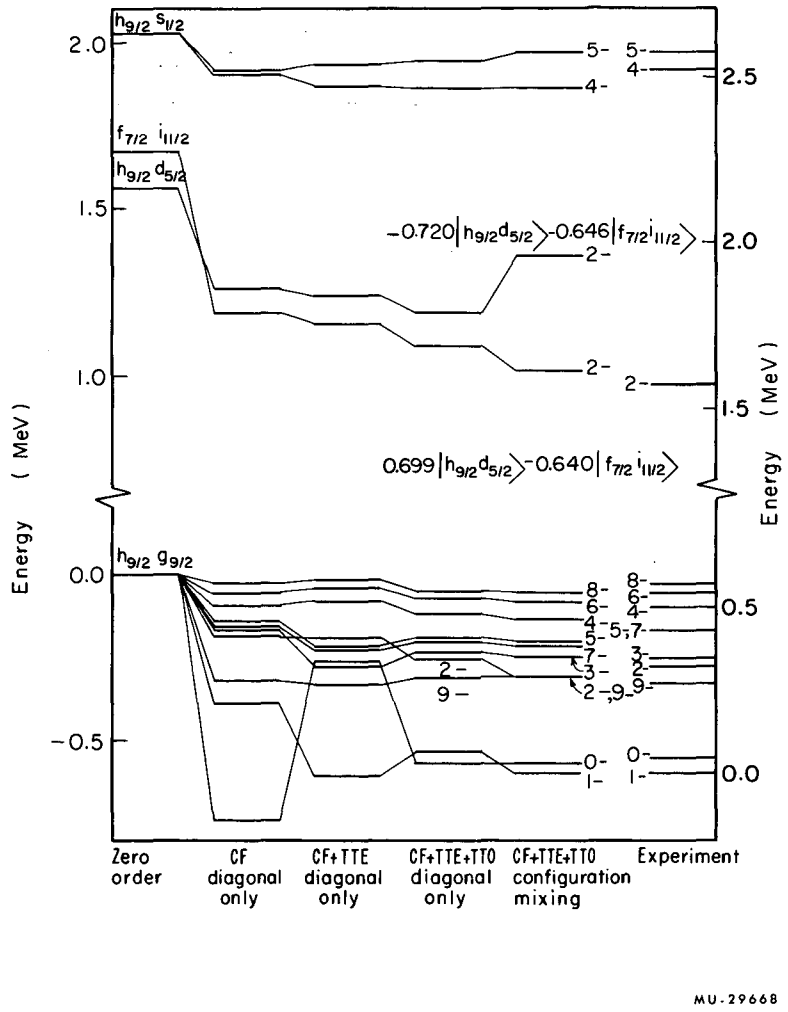

Fig. 8. Comparison of the experimental and calculated spectra of Bi^{210} with the slightly modified residual force. The symbols CF, TTE, and TTO refer to the central, tensor-even, tensor-odd forces, respectively.

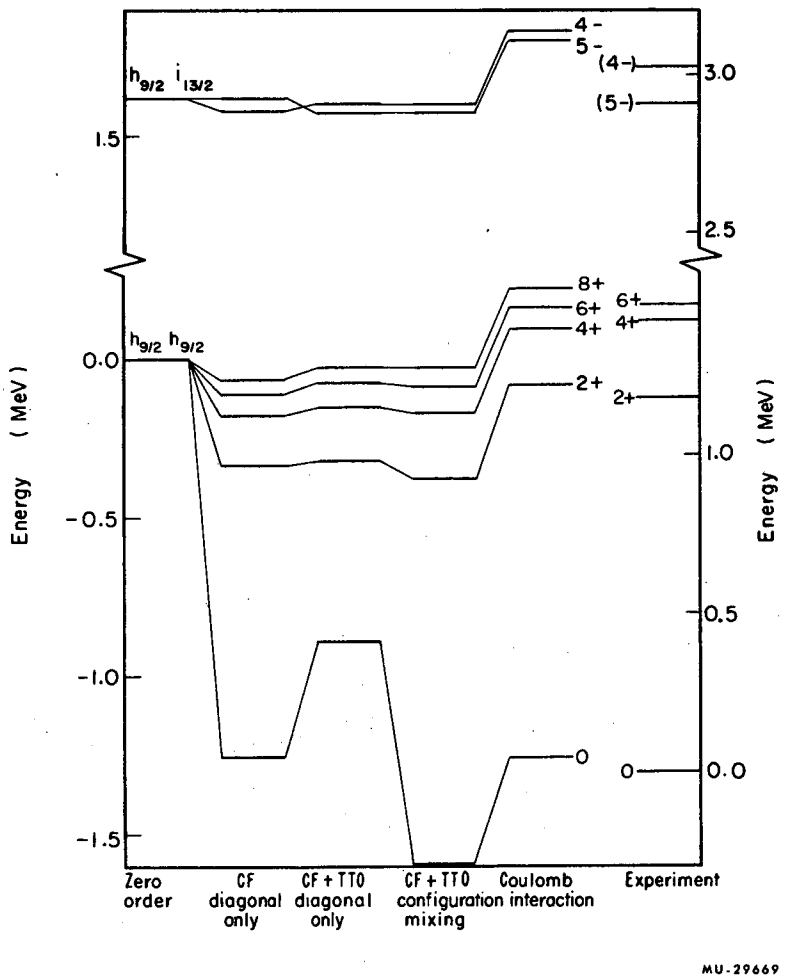

Fig. 9. Comparison of the experimental and calculated spectra of Po^{210}. The abbreviations CF, TTE, and TTO refer to the central, tensor-even, and tensor-odd forces, respectively.

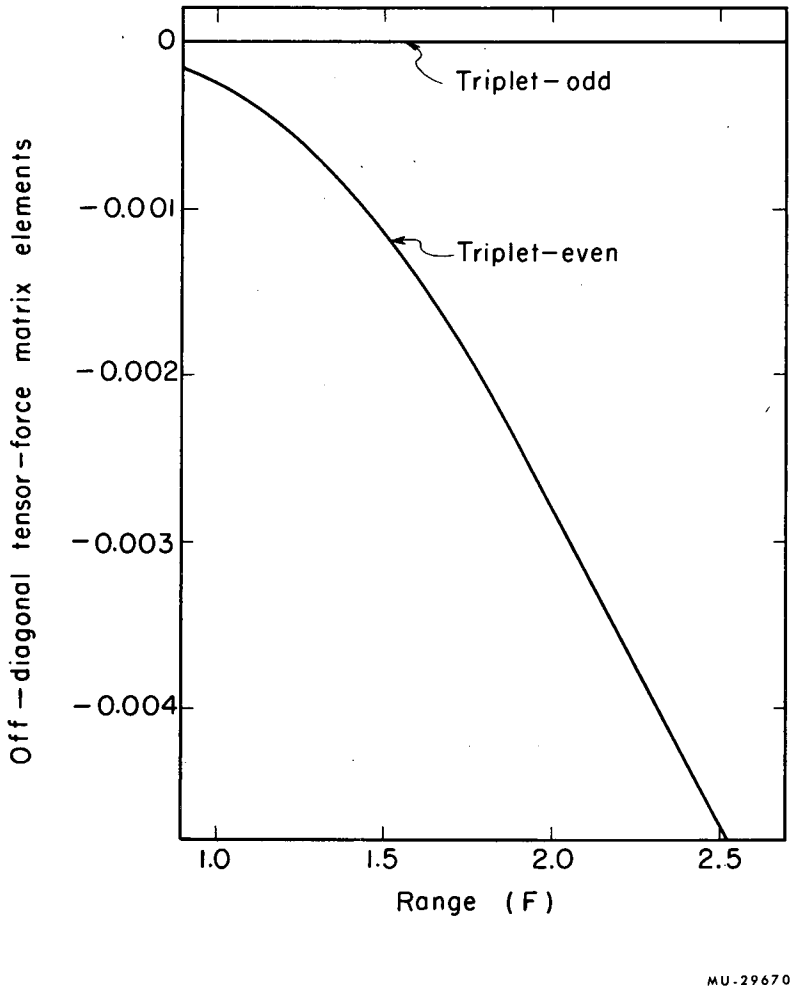

Fig. 10. Off-diagonal tensor-force matrix elements $(1/3)\langle h_{9/2}\ g_{9/2}|P_{TE}\ U^{T}_{TE}\ S_{12}|h_{9/2}\ i_{11/2}\rangle$ and $(1/3)\langle h_{9/2}\ g_{9/2}|P_{TO}\ U^{T}_{TO}\ S_{12}|h_{9/2}\ i_{11/2}\rangle$ for Bi^{210} as a function of the force range.

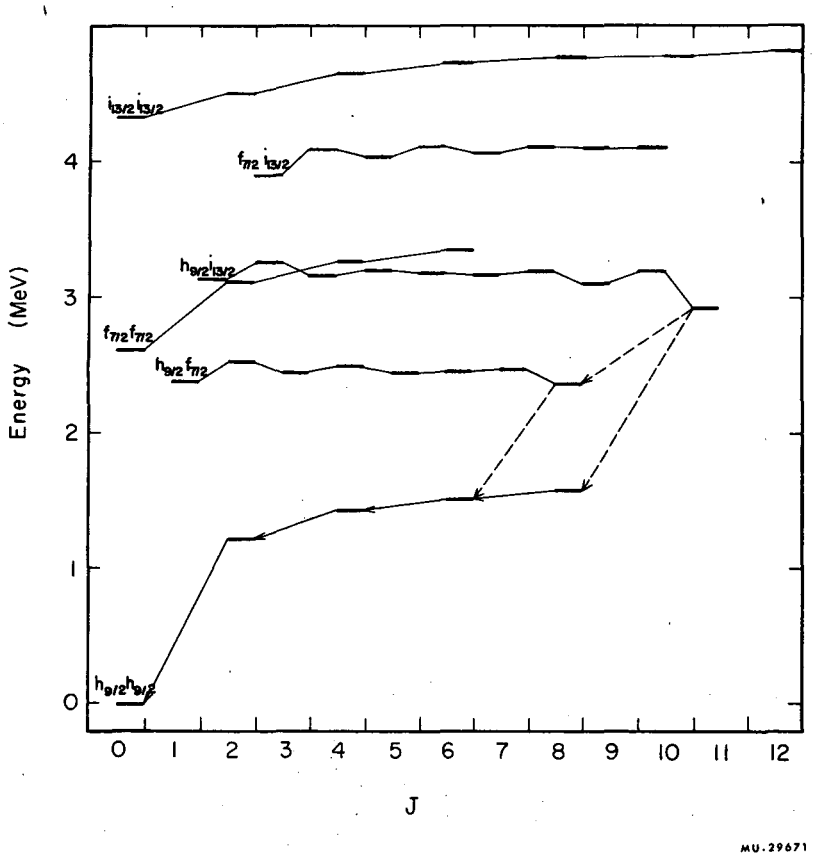

Fig. 11. Calculated energy levels of Po^{210}. For each spin, the left column lists the odd-parity states and the right column the even-parity states. The various spin-J states arising from the same configuration are connected by lines, and the possible E3 and E2 transitions from the predicted isomeric state $(h_{9/2}\ i_{13/2})^{J=11-}$ are shown by arrows and dashed lines.